Data in brief 23 (2019) 103749

Contents lists available at ScienceDirect

Data in brief

journal homepage: www.elsevier.com/locate/dib

Data Article

Dataset on the bearing capacity of curved profiles obtained by roll forming process

Silvia Caprili [a, *], Christian Fauth [b], Irene Puncello [a, *], Daniel C. Ruff [b], Walter Salvatore [a], Thomas Ummenhofer [b]

[a] *University of Pisa, Italy*
[b] *Karlsruhe Institute of Technology (KIT), Germany*

A R T I C L E I N F O

Article history:
Received 2 January 2019
Received in revised form 1 February 2019
Accepted 5 February 2019
Available online 7 March 2019

A B S T R A C T

The paper shows experimental data concerning the bearing capacity of curved profile sheets achieved by roll forming process. Two different restraint configurations were considered, respectively named A and B and representing the only bending and the axial-bending conditions. Two different experimental setup, i.e. single span with and without horizontal restraints were adopted. Trapezoidal and sinusoidal steel sheets with variable thickness and curvature radius were tested. Setup configurations, collapse mechanisms and load-deflection diagrams are presented.

Specifications table

Subject area	*Engineering*
More specific subject area	*Design of steel structure*
Type of data	*Table, figures, diagrams*
How data was acquired	*Displacement were acquired through jack and sensors. Forces were acquired through load cells*
Data format	*Analysed*
Experimental factors	*The profiles used for the tests were achieved through roll forming process of flat steel sheets. Flat specimens were also considered for comparison.*
Experimental features	*Load-deflection diagrams, failure load values for each experimental configuration, pictures representing setup and collapse mechanism.*

* Corresponding authors.
E-mail addresses: silvia.caprili@ing.unipi.it, irene.puncello@ing.unipi.it (I. Puncello).

https://doi.org/10.1016/j.dib.2019.103749

Data source location	*KIT Steel & Lightweight Structures at Research Center for Steel, Timber and Masonry, Germany, Europe*
Data accessibility	*Data is with the article*
Related research report	*Prudor V., Izabel D., Vienne M., Holz R., Renaux T., Fauth C., Palisson A. Guidelines and Recommendations for Integrating Specific Profiled Steel Sheets in the Eurocodes (GRISPE). Report EUR 28913 EN. European Commission, Directorate-General for Research and Innovation. Directorate D — Industrial Technologies, Unit D.4 — Coal and Steel. 2017.*

Value of the data

- The load-deflection diagrams can be used to compare the behaviour of the tested specimens with profiles characterized by different curvature radius, thickness, geometry, etc.
- Data coming from experimental tests on curved profiles can be compared to flat ones, allowing to determine differences and giving useful and simple design indications.
- Data can be used to understand how different curvatures can alter the bearing capacity of curved profiles, comparing them to flat ones.
- Data can be used to elaborate simple rules for the assessment of the bearing capacity of curved profiles.

1. Data

Curved profile steel sheets are widely used for engineering and architectural applications, allowing to provide high performing solutions and good aesthetic requirements. By the way, current European design standards for steel structures do not provide any indication concerning how to determine the bearing capacity of such kind of profiles, limiting their practical adoption. A wide experimental test campaign was performed within the framework of the positively concluded European project GRISPE "*Guidelines and recommendations for integrating specific profiled steel sheets in the Eurocodes*" funded by the Research Fund for Coal and Steel (RFCS-CT-2013-0018). Experimental tests aimed to determine the bearing capacity of curved profile steel sheets, with reference to the 'original' flat condition. In the present paper, data achieved from the above-mentioned experimental campaign are presented.

Tests were performed at the Karlsruhe Institute of Technology (KIT – Germany) on two different typologies of curved specimens, obtained by roll forming process: the corrugated sheets produced by Bacacier® and the trapezoidal sheets manufactured by Arcelor Mittal Construction France were studied. The experimental test campaign was performed with the aim to develop new simple methodologies for the design of curved profile sheets with different geometrical and mechanical characteristics and restraint conditions, comparing them with methods used for flat sheets.

Table 1 summarizes the main characteristics of considered steel sheet specimens, in terms of materials and geometry of the source flat samples (Fig. 1 and Fig. 2). Two different thicknesses were considered, respectively equal to 0.63 mm and 1.00 mm; different curvature radii (R) were applied resulting in profiles with variable geometry in terms of length (b) and maximum mid-span deflection (f) (Fig. 3).

Table 1
Characteristics of the specimens.

Type of profile	Steel grade according to EN 10346:2009	Height [mm]	Width [mm]	Thickness [mm]
Bacacier 18/76	S320GD	18	912	0.63 and 1.00
Arcelor Mittal 39/333	S320GD	39	1000	0.63 and 1.00

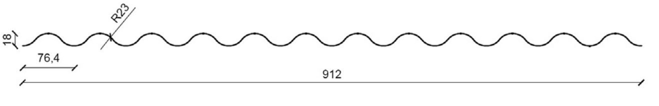

Fig. 1. Cross section of the sinusoidal profile 18/76.

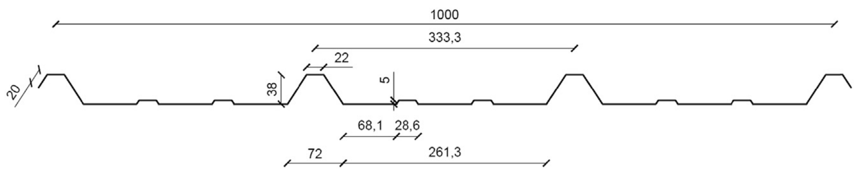

Fig. 2. Cross section of the trapezoidal profile 39/333.

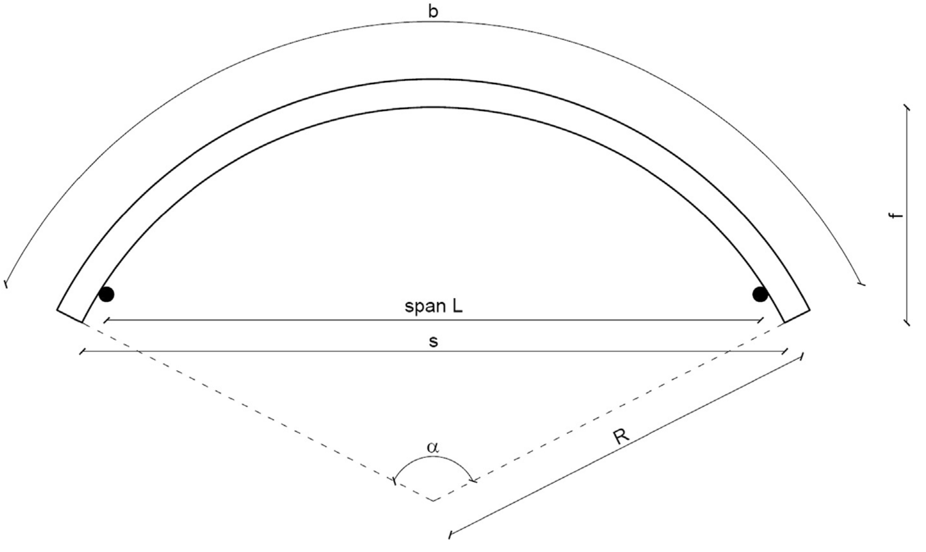

Fig. 3. Characteristic parameters of curved profiles.

2. Experimental design, materials and methods

2.1. Experimental test setups

Experimental tests were performed using two different configurations representing two different stress conditions, in the following respectively called *Configuration A* and *Configuration B*. Configuration A refers to single span tests without horizontal restraints: in this conditions, curved profile sheets are subjected only to bending actions. In Configuration B, single span specimens present horizontal restraints: curved steel sheets are then subjected to combined bending moment and axial force, behaving like an arch. The overall test setup is presented in Fig. 4.

In both configurations, the uniformly distributed pressure load condition was reproduced through a system of transverse steel sections and timber blocks. The load was introduced into the valleys of the corrugated sheets or into the bottom flanges of the trapezoidal ones through four lines loads located at 0.125, 0.375, 0.625, 0.875 of the span length, in a symmetric configuration. Due to the isostatic load distribution system, the 4 line-loads are equal.

The transverse steel sections were clamped to the profile; oil was used to reduce the friction between the transverse steel beams at the supports of the load distribution system. The load was applied in displacement control by monitoring the vertical deflection of the sheet; deflections were measured by two trip wire displacement sensors placed in the mid-span under the bottom flanges.

The speed application ranged between 6 and 15 mm/min; a cell load with a maximum capacity of 50 kN was used.

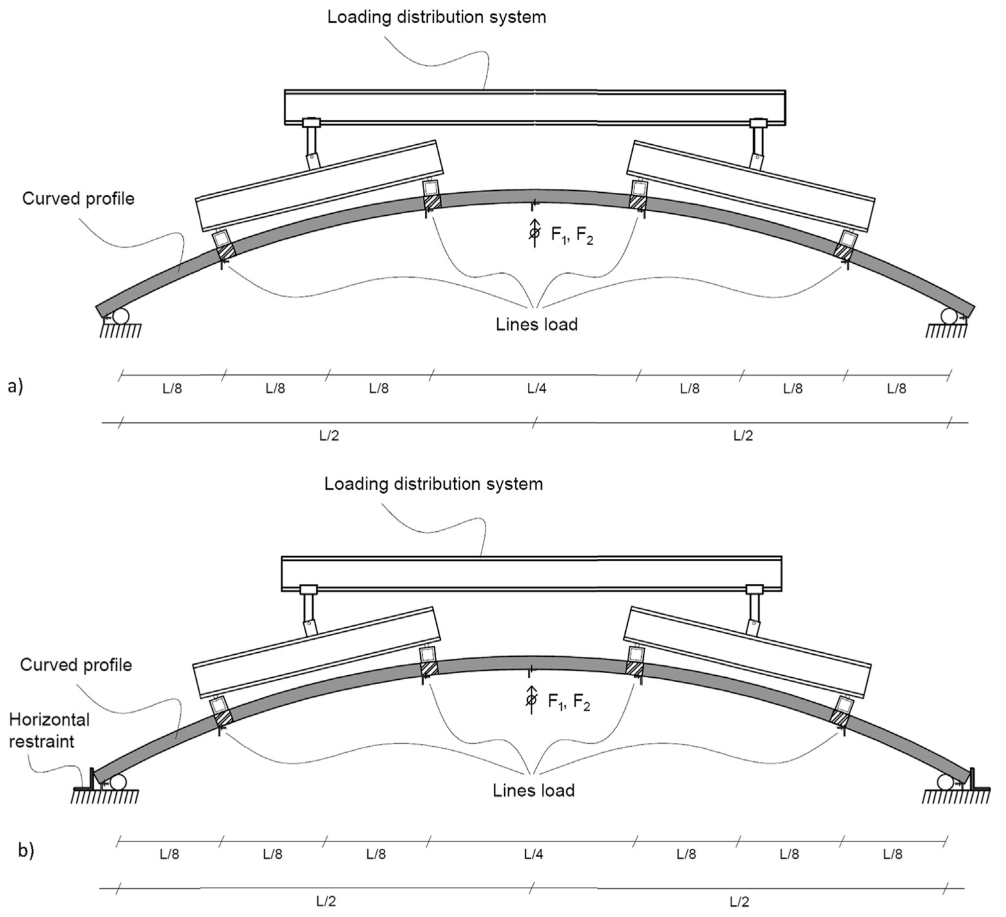

Fig. 4. Overall experimental setup adopted for the experimental tests: a) single span test without horizontal restraints; b) single span test with horizontal restraints.

In the case of Configuration A (Fig. 4a), the specimens were free to move in the horizontal direction. No axial forces (or, in general negligible values of axial forces) appeared in cross-section in the middle of the span, where the bending moment reached its maximum value. The presence of the horizontal restraints in Configuration B (Fig. 4b), on the other hand, leads to additional axial forces in cross section whereby an arch support effect arises. Thus, bending moments and axial forces act in the cross section in the middle of the span. In Configuration B the static system of the test specimen is hyperstatic: the internal forces do not depend only from the applied load but also from the stiffness parameters of the beam and its supports. The statistic evaluation is applied on the failure loads to determine an individual characteristic (failure) load for each subset.

The ratios among bending moment and axial compression varied according to the curvature of the specimen. Fig. 5, Fig. 6 and Fig. 7 show the test setup adopted for the two different types of steel sheet in the two different flat and curved configurations (A, B).

2.2. Tested specimens

Both sinusoidal and trapezoidal curved sheets of thickness equal to 0.63 and 1.00 mm were tested adopting Configuration A. For the combined bending and axial condition (Configuration B) only trapezoidal curved profiles with thickness equal to 0.63 mm were used. Table 2 summarizes the main

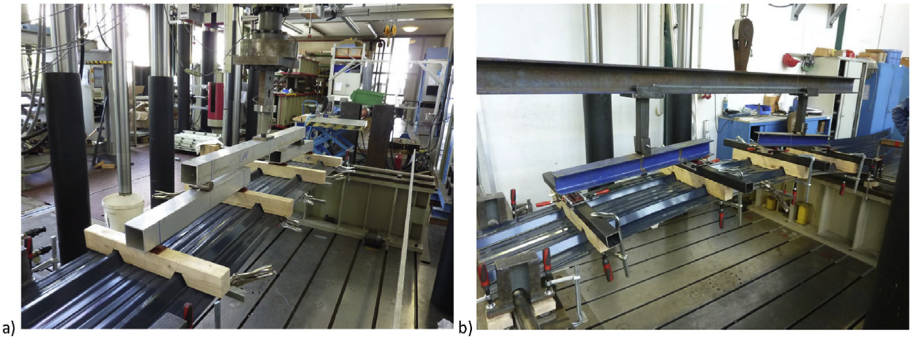

Fig. 5. Single span test setup for trapezoidal sheets profile (39/333): a) flat profile, b) curved profile. Configuration A.

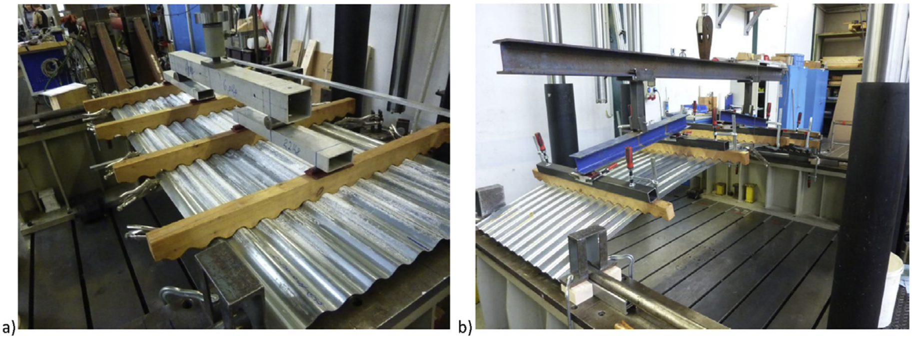

Fig. 6. Single span test setup for sinusoidal sheets profile (18/76): a) flat profile, b) curved profile. Configuration A.

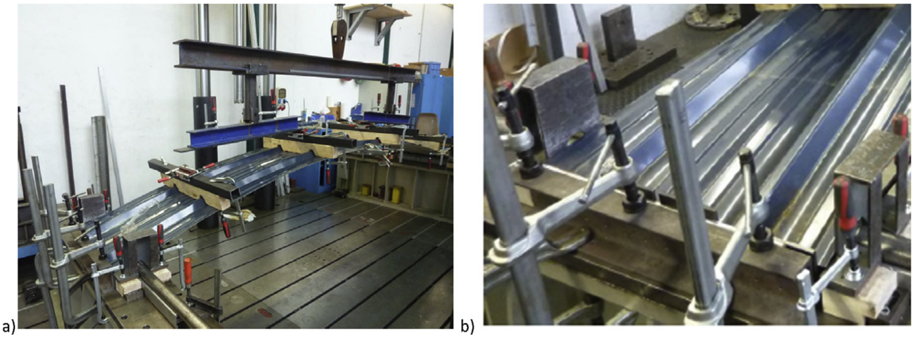

Fig. 7. Single span test setup for curved trapezoidal sheets profile (39/333). Configuration B.

characteristics of tested specimens, being '*R*' the curvature radius of the curved profile, '*b*' its resulting length, '*L*' the distance between supports and '*s*' the horizontal length and '*f*' the maximum height of the curved profile, as simply presented in Fig. 3.

The effective radius of curvature differs from the designed value, due to tolerances in the curving process. The real height of the arch in correspondence of the two ends was then measured, adopting the mean value to identify the real 'R'. Since the spread among the heights of the test family is small, the mean radius is considered representative for all the specimens of the same family.

Table 3 summarizes the effective geometry of tested specimens. For each specimens a specific tag including the typology of profile (18 – sinusoidal; 39 – trapezoidal), the height of the profile (f) and the

Table 2
Main characteristics of tested specimens.

Configuration	Profile	R (mm)	B (mm)	L (mm)	s (mm)	f (mm)	α (°)	n. tests
A	18/76 $t_N = 0.63$ mm	∞	2200	2000	2200	0	0	3
		20	2201			30	6.31	2
		10	2204			61	12.63	2
		4	2229			154	31.92	2
	18/76 $t_N = 1.00$ mm	∞	3200	3000	3200	0	0	1
		20	3203			64	9.18	4
		10	3214			129	18.41	3
		4	3292			334	47.16	3
	39/333 $t_N = 0.63$ mm	∞	3200	3000	3200	0	0	3
		20	3203			64	9.18	2
		10	3214			129	18.41	2
		6	3239			217	30.93	3
	39/333 $t_N = 1.00$ mm	∞	4200	4000	4200	0	0	2
		20	4208			111	12.05	2
		10	4232			223	24.24	2
		6	4291			380	40.98	2
B	39/333 $t_N = 0.63$ mm	6	3239	3000	3200	217	30.93	2
		6	4291	4000	4200	380	40.97	3
		6	5300	5000	5129	576	50.61	3

Table 3
Effective geometry of the curved profile sheets.

Test spec.	Span	Height of the arch			Radius (m)	Slope at support
	L (m)	left side	right side	Mean value	Mean value	α/2 (arc)
18-30-063-1	2	40	47	43.8	11.50	0.087
18-30-063-2		40	48			
18-61-063-1	2	45	56	52.3	9.60	0.104
18-61-063-2		48	60			
18-154-063-1	2	120	115	118.8	4.30	0.236
18-154-063-2		120	120			
18-64-100-1	3	75	60	65.5	17.20	0.087
18-64-100-2		70	70			
18-64-100-3		64	60			
18-64-100-4		60	65			
18-129-100-1	3	110	120	106.7	10.60	0.142
18-129-100-2		110	125			
18-129-100-3		90	85			
18-334-100-1	3	320	300	309.2	3.80	0.407
18-334-100-2		325	295			
18-334-100-3		315	300			
39-64-063-1	3	37	34	34.3	32.90	0.046
39-64-063-2		34	32			
39-129-063-1	3	116	116	117.0	9.70	0.156
39-129-063-2		116	120			
39-217-063-1	3	205	200	205.8	5.60	0.273
39-217-063-2		205	205			
39-217-063-3		210	210			
39-111-100-1	4	74	82	77.5	25.80	0.077
39-111-100-2		74	80			
39-223-100-1	4	190	190	190.0	10.60	0.189
39-223-100-2		190	190			
39-380-100-1	4	320	327	321.8	6.40	0.319
39-380-100-2		325	315			
H-39-217-063-1	3	200	210	206.3	5.56	0.273
H-39-217-063-2		205	210			
H-39-380-063-1	4	330	350	341.7	6.02	0.338
H-39-380-063-2		340	350			
H-39-380-063-3		335	345			
H-39-576-063-1	5	460	465	459.2	7.04	0.363
H-39-576-063-2		450	455			
H-39-576-063-3		460	465			

Table 4
Results of experimental tensile tests for material properties.

Profile	Nominal Thickness	Core Thickness	Yield Strength	Tensile Strength	Ultimate elongation
	t_N (mm)	t_K (mm)	$R_{p,02}$ (MPa)	R_m (MPa)	$A_{L=80\ mm}$ (%)
18/76	0.63	0.53	330	456	26.2
		0.53	329	457	26.0
		0.52	329	456	25.4
	1.00	0.99	342	387	29.3
		1.00	346	387	27.6
		0.99	358	392	27.9
39/333	0.63	0.58	406	430	27.6
		0.58	411	430	26.4
		0.58	408	431	27.0
	1.00	0.96	379	425	24.7
		0.96	384	427	24.5
		0.95	382	426	25.4

thickness was adopted. The leading character “H” in the test's designation indicates tests performed in Configuration B (with horizontal restraints).

2.3. Material properties

The tested profiles were produced from coils consisting of steel grade S320 GD according to EN 10346:2015 [1]. Tensile tests were executed on 3 specimens per sheet and per thickness to determine the material properties, following the indication provided by EN 6892-1:2009 [2]. In the case of trapezoidal sheets, the specimens have been cut out from the tested sheets while in the case of sinusoidal sheets the producer provided the specimens, with the specimen shape 2 according to EN 6892-1:2009 [2] Table B1. The determination of the yield strength $R_{p0.2}$ and of the ultimate tensile strength R_m was based upon the measured sheet thickness exclusive of zinc coating. Data achieved are summarized in Table 4.

2.4. Experimental results

Test series, included specimens analysed adopting the same setup and showing the same failure modality, were analysed. Each test series consisted, moreover, of several subsets: a subset is a small series of tests with identical conditions (same profile type, same nominal sheet thickness, same test setup etc.). A subset usually consisted of 2 or 3 identical tests.

As a general remark, tests performed in Configuration A mainly evidenced failure by bending. In the case of Configuration B (bending moment and axial force) failure occurred due to a combination of global buckling and bending. Data achieved from tests performed in Configuration A are summarized in Table 6 and in.

Table 7 respectively for sinusoidal (18/76) and for trapezoidal profiles (39/333). The maximum load (F_{max}) represents the failure load including preload and neglecting the self-weight of the specimen.

A statistical evaluation of experimental data - performed taking into consideration the procedure provided by EN 1993-1-3 (table A2) [3] for the determination of coefficient - was used to evaluate the characteristic values of the bearing properties of curved profiles as follow:

Table 5
Self-weight of the tested profiles.

Profile	Thickness (mm)	Self- weight (kN/m^2)
Bacacier 18/76	0.63	0.059
	1.00	0.093
Arcelor 39/333	0.63	0.060
	1.00	0.095

Table 6
Results of single span test without horizontal restraints in the case of sinusoidal profiles (18/76).

Test specimen		Span (mm)	t_N (mm)	b (mm)	L_V (mm)	Measured t_N including zinc coating (mm)	Measured f (mm)		Measured b (mm)	Preload (kN)	F_{max} (kN)	$F_{u,k}$ (kN)	$M_{c,Rk,F}$ kNm/m
18-0-063-1	(1)	2000	0.63	2200	2200	0.57	0	0	894	0.29	3.71	4.112	1.057
18-0-063-2	(1)				2200	0.56	0	0	895		4.07		
18-0-063-3	(1)				2200	0.56	0	0	890		3.91		
18-30-063-1	(1)			2201	2200	0.59	40	47	890	0.29	3.97	4.168	1.071
18-30-063-2	(1)				2200	0.55	40	48	892		3.93		
18-61-063-1	(1)			2204	2200	0.56	45	56	888	0.49	4.11	4.284	1.100
18-61-063-2	(1)				2200	0.56	48	60	890		4.01		
18-154-063-1	(2)			2229	2200	0.56	120	115	890	0.49	4.98	5.192	1.327
18-154-063-2	(2)				2200	0.55	120	120	895		4.86		
18-0-100-1	(1)	3000	1.00	3200	3200	1.00	0	0	887	0.35		4.326	1.727
18-64-100-1	(2) *			3203	3200	0.99	75	60	885	0.49	4.20	4.353	1.736
18-64-100-2	(2) *				3200	0.99	70	70	885		4.10		
18-64-100-3	(2) *				3200	0.99	64	60	885		4.10		
18-64-100-4	(2) *				3200	0.99	60	65	885		4.10		
18-129-100-1	(2) *			3214	3200	1.01	110	120	885	0.49	4.00	4.186	1.674
18-129-100-2	(2) *				3200	1.00	110	125	885		4.00		
18-129-100-3	(2) *				3200	0.99	90	85	885		3.90		
18-334-100-1	(2) *			3292	3200	1.00	320	300	885	0.8	3.80	4.151	1.661
18-334-100-2	(2) *				3200	1.00	325	295	885		4.00		
18-334-100-3	(2) *				3200	1.00	315	300	885		4.00		

In the table, the apex (1) identifies the test setup for flat profiles and the apex (2) identifies the test setup for curved profiles.
The apex * identifies the specimens which reach collapse for plastic deformation, in the other cases the collapse is due to local buckling phenomena.

Table 7
Results of single span test without horizontal restraints in the case of trapezoidal profiles (39/333).

Test		Span (mm)	t_N (mm)	b (mm)	L_V (mm)	Measured t_N including zinc coating (mm)	Measured f (mm)		Measured b (mm)	Preload (kN)	F_{max} (kN)	$F_{u,k}$ (kN)	$M_{c,Rk,F}$ kNm/m
39-0-063-1	(1)	3000	0.63	3200	3200	0.66	0	0	668	0.43	2.09	1.915	0.785
39-0-063-2	(1)				3200	0.65	0	0	660		2.03		
39-0-063-3	(2)				3200	0.65	0	0	670		1.85		
39-64-063-1	(1)			3203	3200	0.66	37	34	660	0.4	1.92	1.867	0.767
39-64-063-2	(1)				3200	0.66	34	32	663		1.96		
39-129-063-1	(1)			3214	3200	0.65	116	116	663	0.43	1.84	1.776	0.733
39-129-063-2	(1)				3200	0.65	116	120	661		1.85		
39-217-063-1	(2)			3239	3200	0.64	205	200	670	0.48	1.61	1.546	0.647
39-217-063-2	(2)				3200	0.66	205	205	670		1.56		
39-217-063-3	(2)				3200	0.68	210	210	668		1.65		
39-0-100-1	(1)	4000	1.00	4200	4200	1.02	0	0	665	0.49	2.8	2.699	1.539
39-0-100-2	(1)				4200	1.01	0	0	668		2.81		
39-111-100-1	(1)			4208	4200	1.01	74	82	668	0.71	2.78	2.646	1.513
39-111-100-2	(1)				4200	1.02	74	80	668		2.72		
39-223-100-1	(2)			4232	4200	1.02	190	190	670	0.49	2.81	2.709	1.544
39-223-100-2	(2)				4200	1.03	190	190	670		2.82		
39-380-100-1	(2)			4291	4200	1.03	320	327	670	0.49	2.82	2.728	1.554
39-380-100-2	(2)				4200	1.04	325	315	670		2.85		

In the table, the apex (1) identifies the test setup for flat profiles and the apex (2) identifies the test setup for curved profiles. The collapse of the specimens is due to local buckling phenomena.

$$R_k = R_m \cdot (1 - k \cdot s)$$

Being:
R_m mean value of tensile stress of the subset.
s standard deviation.
k coefficient depending on the test number, according the table A2 provided by EN 1993-1-3 [3].

For tests performed according to Configuration A, the characteristic bending moment in span was determined as follow:

$$M_{c,Rk,F} = \frac{F_{u,k}}{b_V} \cdot \frac{L}{8} + g \cdot L_V \cdot \frac{(2L - L_V)}{8}$$

Being:
$F_{u,k}$ the characteristic load in kN (including preload).
b_V the width of the test specimen (this parameter has a value of, respectively, 912 and 1000 mm in case profile's thickness equal to 0.63 mm and 1.00 mm).
L_V the length of the test specimen.
L the span length.
g the self-weight of the test specimen, determined according to Table 5

In case of sinusoidal sheets, the collapse occurred due to local buckling in correspondence of the crest for thickness equal to 0.63 mm; plastic deformations were otherwise evidenced in the case of 1.00 mm thickness. Trapezoidal sheets evidenced collapse due to local buckling of the upper flange (Table 7). Pictures of the different failure modes are presented in Figs. 8–13 (see Fig. 14).

In the following diagrams (Fig. 14), the relations among load and displacement are depicted for some of the executed tests. For each test two different curves are represented, since the displacement has been measured in two different points: in correspondence of the midspan sensor and in correspondence of the jack.

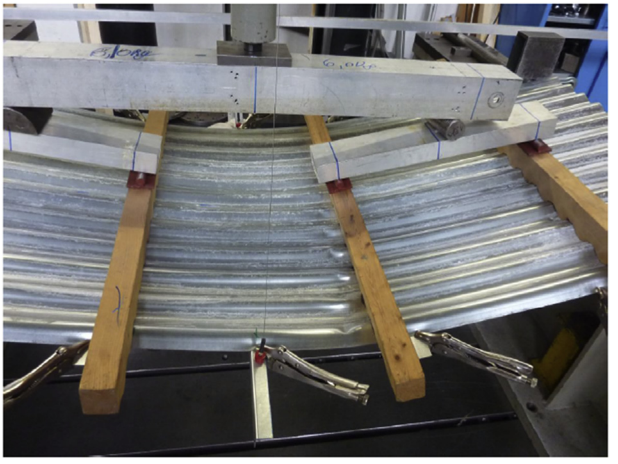

Fig. 8. Failure mode (local buckling) of curved sinusoidal sheets profile (18/76), thickness 0.63 mm. Configuration A.

Fig. 9. Failure mode (plastic deformation) of curved sinusoidal sheets profile (18/76), thickness 1.00 mm. Configuration A.

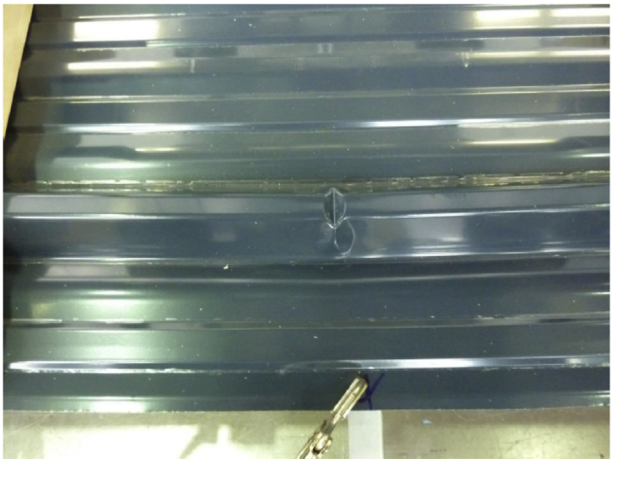

Fig. 10. Failure mode (local buckling of the upper flange) of curved trapezoidal sheets profile (39/333), thickness 0.63 mm. Configuration A.

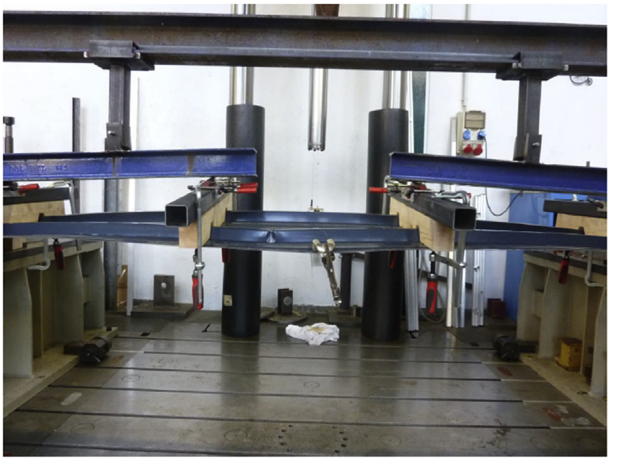

Fig. 11. Failure mode (local buckling of the upper flange) of curved trapezoidal sheets profile (39/333), thickness 0.63 mm. Configuration A.

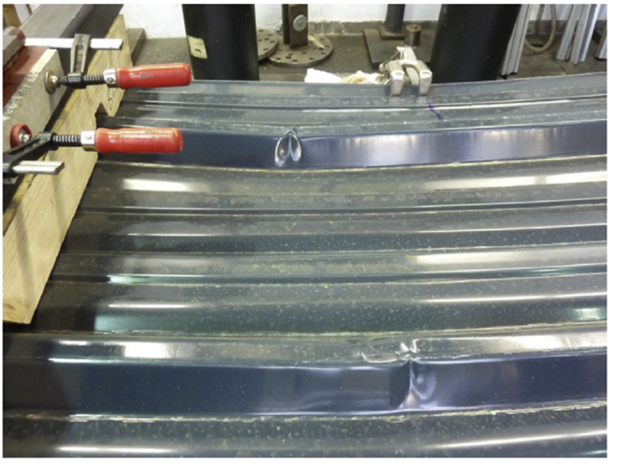

Fig. 12. Failure mode (local buckling of the upper flange) of curved trapezoidal sheets profile (39/333), thickness 1.00mm. Configuration A.

Data achieved from Configuration B (tests with horizontal restraints) are summarized in Table 8 for trapezoidal profiles (39/333). Once again, F_{max} represents the failure load including preload but without considering the self-weight of the tested specimen. Pictures of the different failure modes are presented in Figs. 15–20.

In the following diagrams (Fig. 21) the relations among load and displacement are depicted for some of the executed tests. For each test two different curves are represented, since the displacement has been measured in two different points: in correspondence of the midspan sensor and in correspondence of the jack.

In the following diagrams, the relations among load and displacement are depicted for some of the executed tests. For each test two different curves are represented, since the displacement has been measured in two different points: in correspondence of the midspan sensor and in correspondence of the jack.

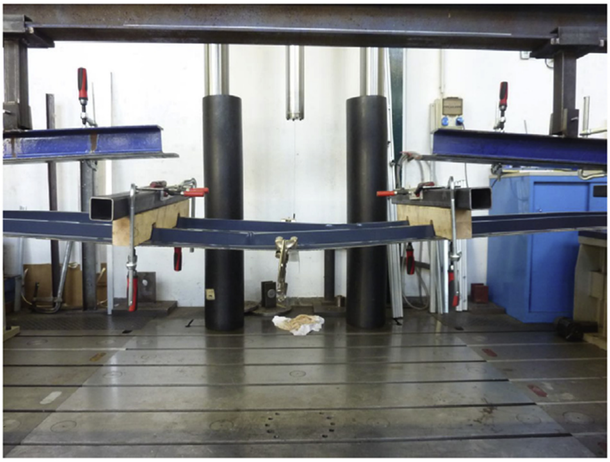

Fig. 13. Failure mode (local buckling of the upper flange) of curved trapezoidal sheets profile (39/333), thickness 1.00mm. Configuration A.

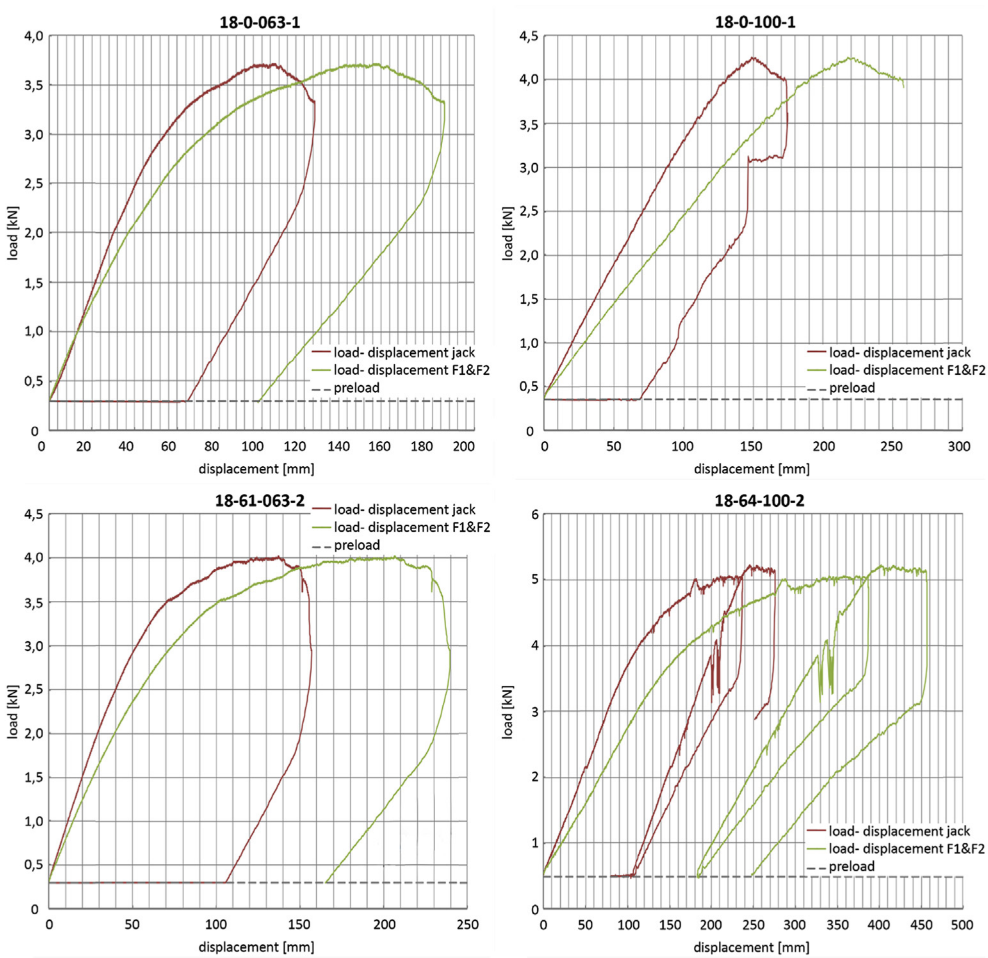

Fig. 14. Load-midspan deflection diagrams derived from some of the executed experimental tests – Configuration A. The test TAGS correspond to Tables 6 and 7.

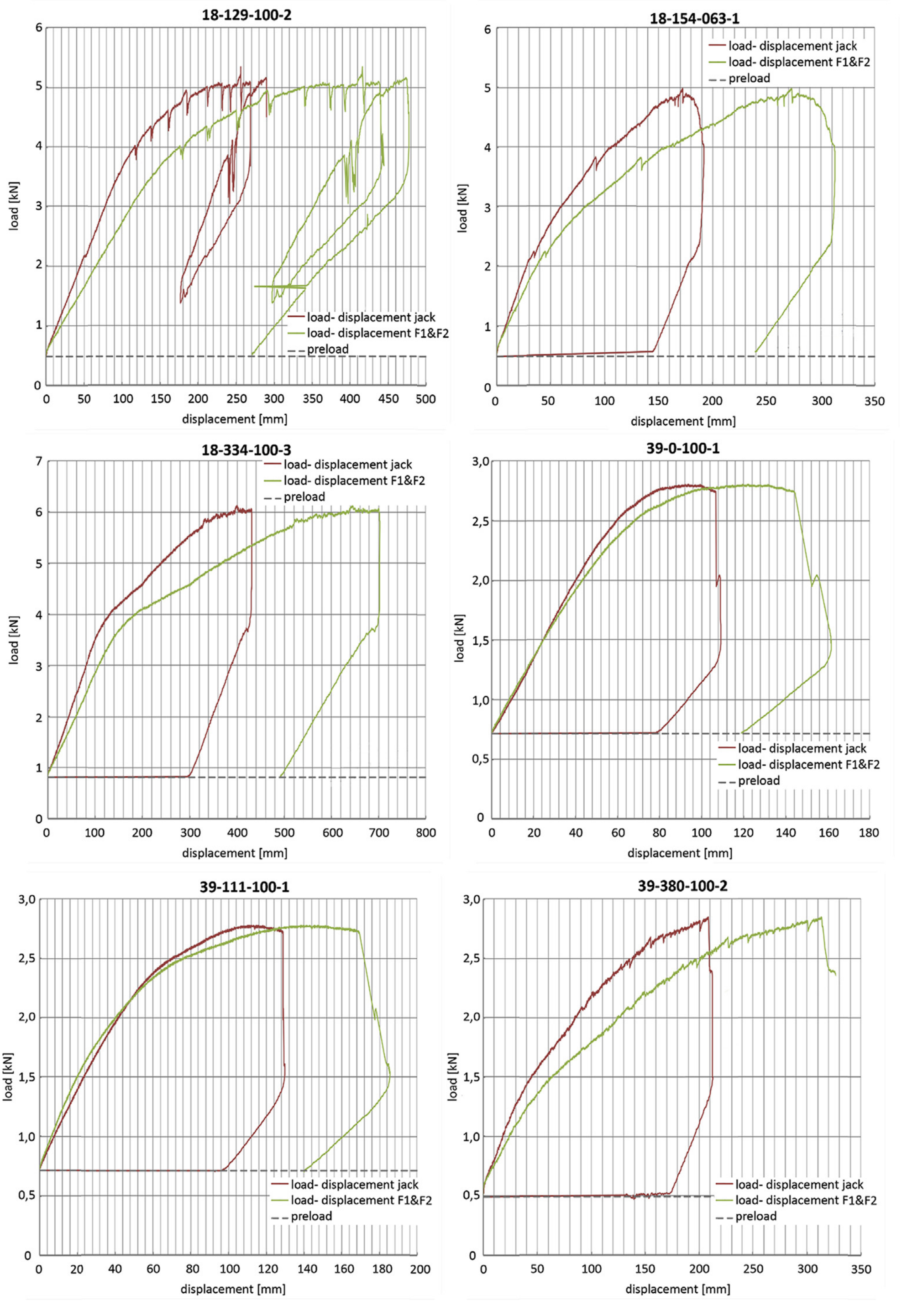

Fig. 14. *continued*

Table 8
Results of single span test with horizontal restraints of trapezoidal profiles (39/333) — Configuration B. In the table, the apex *(1)* identifies the test setup for curved profiles.

Test	Span (mm)	t_N (mm)	b (mm)	L_V (mm)	Measured t_N including zinc coating (mm)	Measured f (mm)		Measured b (mm)	Preload (kN)	F_{max} (kN)	$F_{u,k}$ (kN)
H-39-217-063-1 (1)	(mm)	0.63	(mm)	3200	0.66	200	210	670	0.49	9.12	11.027
H-39-217-063-2 (1)		0.63	3239	3200	0.66	205	210	670		8.95	
H-39-380-063-1 (1)	4000	0.63	4239	4200	0.66	330	350	670	0.49	9.49	12.767
H-39-380-063-2 (1)		0.63	4239	4200	0.66	340	350	670		11.43	
H-39-380-063-3 (1)		0.63	4239	4200	0.66	335	345	370		11.03	
H-39-576-063-1 (1)	5000	0.63	4291	5200	0.65	460	465	665	0.49	5.67	6.615
H-39-576-063-2 (1)		0.63	4291	5200	0.67	450	455	668		5.17	
H-39-576-063-3 (1)		0.63	4291	5200	0.67	460	465	665		6.83	

In the table, the apex (1) identifies the test setup for curved profiles. The collapse of the specimens is due to local buckling phenomena.

Fig. 15. Detail of plastic deformation occurred at the support. Configuration B.

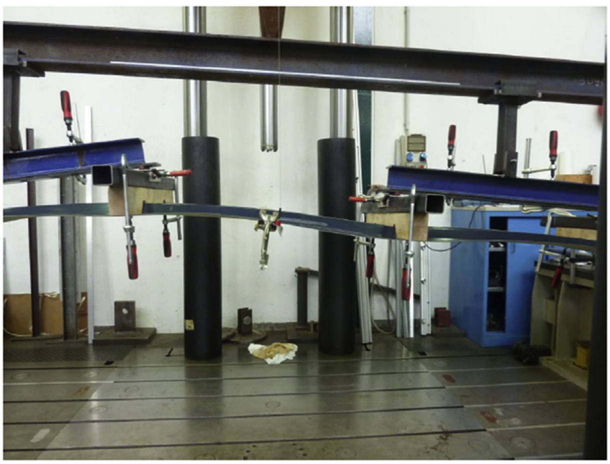

Fig. 16. Failure mode (buckling of the arch) of curved trapezoidal sheets profile (39/333), thickness 0.63mm. Configuration B.

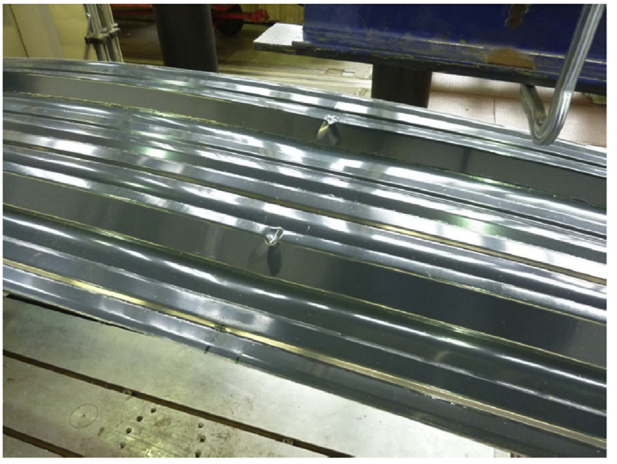

Fig. 17. Failure mode (buckling of the arch) of curved trapezoidal sheets profile (39/333), thickness 0.63mm. Configuration B.

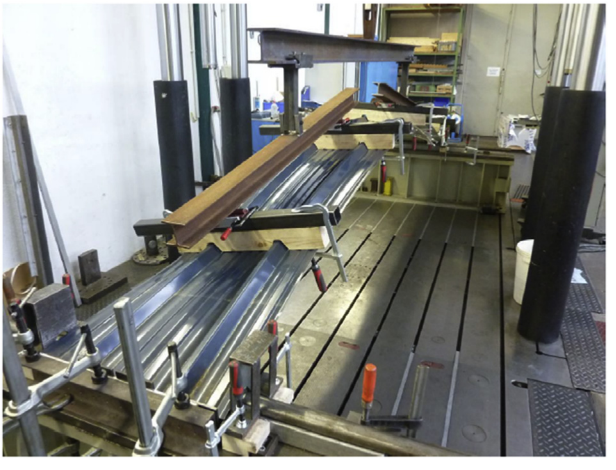

Fig. 18. Side view of the failure mode (buckling of the arch) of curved trapezoidal sheets profile (39/333), thickness 0.63mm. Configuration B.

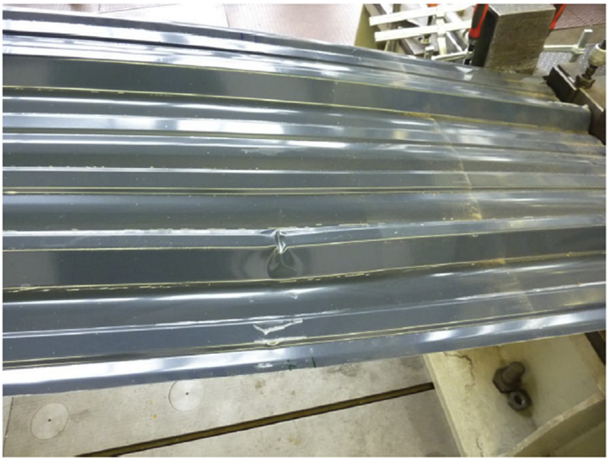

Fig. 19. Detailed view of the failure mode (buckling of the arch) of curved trapezoidal sheets profile (39/333), thickness 0.63mm. Configuration B.

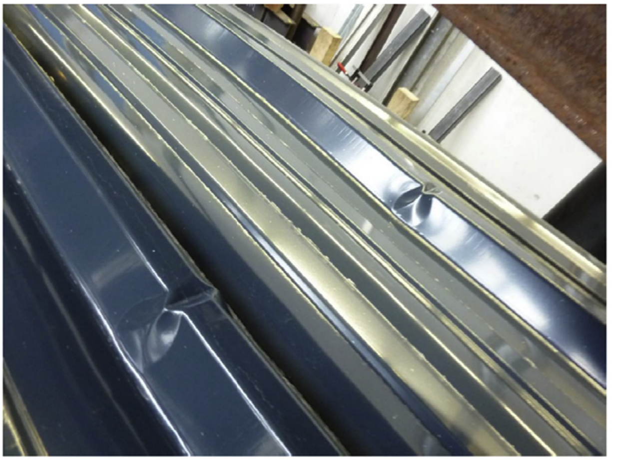

Fig. 20. Detailed view of the failure mode (buckling of the arch) of curved trapezoidal sheets profile (39/333), thickness 0.63mm. Configuration B.

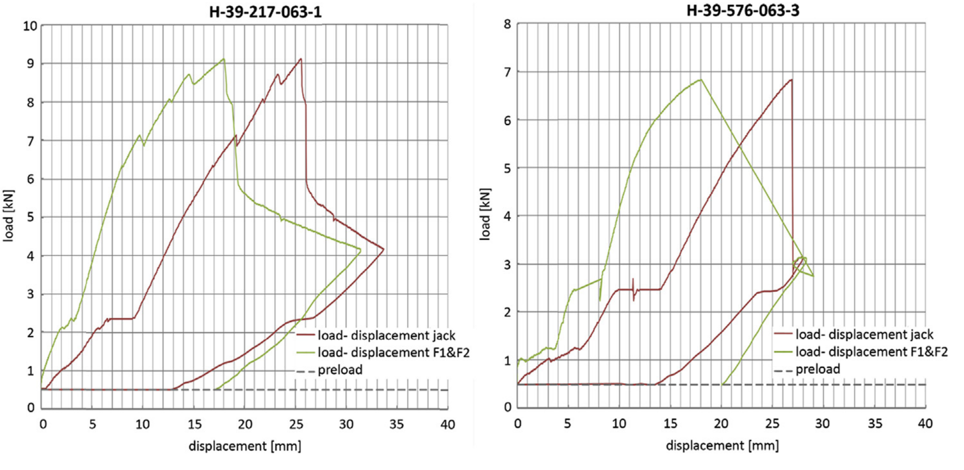

Fig. 21. Load-midspan deflection diagrams derived from some of the executed experimental tests – Configuration B. The test TAGS correspond to Table 8.

Acknowledgements

The present work was developed inside the European Research Project GRISPE "*Guidelines and recommendations for integrating specific profiled steel sheets in the Eurocodes*" co-funded by the Research Fund for Coal and Steel (RFCS-CT-2013-0018). The authors would like to thank all the partners involved in the project for their contributions.

Transparency document

Transparency document associated with this article can be found in the online version at https://doi.org/10.1016/j.dib.2019.103749.

References

[1] UNI EN 10346, Continuously Hot- Dip Coatred Steel Flat Products- Technical Delivery Conditions, 2015.
[2] UNI EN ISO 6892-1, Metallic Materials- Tensile Testing- Part 1: Method of Test at Room Temperature, 2009.
[3] CEN, EN 1993-1-3, Eurocode 3: Design of Steel Structures — Part 1-3: General Rule — Supplementary Rules for Cold-Formed Member and Sheeting, Brussels, 2006, 2006.